

BCS-like superconductivity in $\text{NdO}_{1-x}\text{F}_x\text{BiS}_2$ ($x = 0.3$ and 0.5) single crystals

L. Jiao,¹ Z. F. Weng,¹ J. Z. Liu,² J. L. Zhang,¹ G. M. Pang,¹ C. Y. Guo,¹ F. Gao,¹ X. Y. Zhu,² H. H. Wen,² and H. Q. Yuan^{1,*}

¹Center for Correlated Matter and Department of Physics,
Zhejiang University, Hangzhou, Zhejiang 310027, China

²National Laboratory of Solid State Microstructures and Department of Physics,
National Center of Microstructures and Quantum Manipulation, Nanjing University, Nanjing 210093, China
(Dated: July 21, 2018)

We measure the magnetic penetration depth $\Delta\lambda(T)$ for $\text{NdO}_{1-x}\text{F}_x\text{BiS}_2$ ($x = 0.3$ and 0.5) using the tunnel diode oscillator technique. The $\Delta\lambda(T)$ shows an upturn in the low-temperature limit which is attributed to the paramagnetism of Nd ions. After subtracting the paramagnetic contributions, the penetration depth $\Delta\lambda(T)$ follows exponential-type temperature dependence at $T \ll T_c$. Both $\Delta\lambda(T)$ and the corresponding superfluid density $\rho_s(T)$ can be described by the BCS model with an energy gap of $\Delta(0) \approx 2.0 k_B T_c$ for both $x = 0.3$ and 0.5 , suggesting strong-coupling BCS superconductivity in the presence of localized moments for $\text{NdO}_{1-x}\text{F}_x\text{BiS}_2$.

PACS numbers: 74.70.Xa, 74.25.-q, 74.20.Rp

The newly discovered superconductivity (SC) in $\text{Bi}_4\text{O}_4\text{S}_3$ ^{1,2} and $\text{LnO}_{1-x}\text{F}_x\text{BiS}_2$ ($\text{Ln} = \text{La}, \text{Ce}, \text{Pr}, \text{Nd}$ and Yb)³⁻⁷ has attracted considerable attentions in the community. These compounds crystalize in a layered crystal structure which is composed of an alternative stacking of the BiS_2 double layers and the LnO blocking layer. Electron or hole doping into the LnO layers may induce SC from a semiconducting parent compound⁷. Furthermore, recent measurements revealed a large upper critical field $\mu H_{c2}(0)$ and strong superconducting fluctuations above T_c in some of these superconductors^{8,9}. These features are analogous to those of high T_c cuprates¹⁰ and the iron-based superconductors¹¹ and, therefore, unconventional SC with a possible high T_c transition was expected in the BiS_2 -based compounds. On the other hand, no magnetic order has been revealed in the parent compounds³⁻⁶. Instead, a charge-density-wave (CDW) instability, which favors the conventional electron-phonon pairing mechanism, was theoretically discussed.¹² More recently, coexistence of spin-singlet and spin-triplet pairing states¹³ as well as a g -wave pairing state¹⁴ were proposed for the BiS_2 -based superconductors; the former one arises from the strong spin-orbit coupling while the latter one is presumably driven by electron-electron correlations. Measurements of gap symmetry may provide insights into the above controversies and are, therefore, highly desirable.

Even though intensive efforts have been devoted to the material aspects of this new superconducting family, little work has been done on their superconducting order parameters, which is partially due to the difficult growth of sizable crystals with a high sample quality. Measurements of London penetration depth and the μSR experiments on the polycrystalline $\text{Bi}_4\text{O}_4\text{S}_3$ and $\text{LaO}_{0.5}\text{F}_{0.5}\text{BiS}_2$ ¹⁵⁻¹⁷ showed evidence of an s -wave pairing symmetry. Recently, the successful growth of single crystalline $\text{NdO}_{1-x}\text{F}_x\text{BiS}_2$ provides us a better opportunity to look into its pairing state in more detail^{8,9}. Here we present measurements of the magnetic penetration depth $\lambda(T)$ for $\text{NdO}_{1-x}\text{F}_x\text{BiS}_2$ ($x = 0.3$ and 0.5) single crystals down to 0.4 mK. The penetration depth $\lambda(T)$ and the corresponding superfluid density $\rho_s(T)$ are well described by a single-gap BCS model with strong coupling, providing compelling evidence of s -wave SC for $\text{NdO}_{1-x}\text{F}_x\text{BiS}_2$.

$\text{NdO}_{1-x}\text{F}_x\text{BiS}_2$ ($x = 0.3$ and 0.5) single crystals were grown by using a flux method with CsCl/KCl as flux.⁸ In this context, the F -concentration x refers to the nominal values, which are close to the actual compositions as identified by the energy dispersion spectrum (EDX). Precise measurements of the penetration depth changes $\Delta\lambda(T)$ were performed by utilizing a tunnel-diode oscillator (TDO) based, self-inductive technique at an operating frequencies of 7 MHz down to 0.4 K in a ^3He cryostat, with which we can obtain a noise level as low as 0.01 PPM. The magnetic penetration depth is proportional to the shift of the resonant frequency $\Delta f(T)$, i.e., $\lambda(T) = G\Delta f(T) + \lambda(0)$, where the G factor is solely determined by the sample and coil geometries¹⁸ and $\lambda(0)$ is the penetration depth at zero temperature. The coil of the oscillator generates a tiny ac magnetic field ($\mu_0 H_{ac} \approx 20$ mOe), which is much smaller than the lower critical field of $\text{NdO}_{1-x}\text{F}_x\text{BiS}_2$,¹⁹ ensuring that the measurements were performed in a Meissner state. The electrical resistivity and magnetic susceptibility were measured in a commercial Physical Properties Measurement System (PPMS) and Magnetic Properties Measurement System (MPMS), respectively.

In order to characterize the sample quality, we measured the temperature dependence of the electrical resistivity $\rho(T)$ and magnetic susceptibility $\chi(T)$ for $\text{NdO}_{1-x}\text{F}_x\text{BiS}_2$ ($x = 0.3$ and 0.5), which are presented in Fig. 1. The electrical resistivity shows metallic behavior in the normal state for $x = 0.3$ and $x = 0.5$. The transition temperature T_c , determined from the mid-point of the sharp resistive transitions, is 4.7 K and 4.4 K for $x = 0.3$ and 0.5 , respectively. These T_c values are very close to the onset transition temperature in the magnetic susceptibility $\chi(T)$. A nearly 100% superconducting volume is observed for $x = 0.3$ while it is reduced to 70% for $x = 0.5$. The $\text{NdO}_{1-x}\text{F}_x\text{BiS}_2$ system possesses a very small lower critical field ($\mu_0 H_{c1}(0) \approx 25$ Oe)¹⁹, thus a tiny external magnetic field may significantly broaden the superconducting transition, as shown in Fig. 1(b). The inset of Fig. 1(b) shows the magnetic susceptibility $\chi(T)$ above T_c , which temperature dependence can be fitted by the Curie law. i.e., $\chi(T) = C/T$. The derived Curie constants are $C = 0.0123$ K and 0.0167 K for $x = 0.3$ and 0.5 , respectively. Consequently, an effective moment of $\mu_{eff} \approx 0.31 \mu_B$ and $0.36 \mu_B$ is estimated for $x = 0.3$

and 0.5 respectively, where μ_B is the Bohr magneton. Such Curie behavior seems to extend to the superconducting state as evidenced by the weak upturn of the magnetic susceptibility in the low-temperature limit [see Fig. 1(b)] and is likely attributed to the unpaired magnetic moments of Nd^{3+} ions.

Measurements of the London penetration depth based on the TDO technique provide a unique method to probe the low-temperature excitations without an interference of magnetic field as typically encountered in the μSR and NMR experiments. In Fig. 2, we plot the temperature dependence of the resonant frequency shift $\Delta f(T)$ for $x = 0.3$ and 0.5 with the ac field generated along the c -axis; the inset expands the low-temperature part. In comparison with the magnetic susceptibility data, as shown in Fig. 1, a sharper superconducting transition with $T_c \approx 4.5$ K ($x = 0.3$) and 4.2 K ($x = 0.5$) is observed in $\Delta f(T)$. The so-derived T_c s are close to the corresponding resistive values, and the sharp transition might be related to the absence of magnetic field in the TDO-based measurements. Therefore, the TDO-based measurements can provide a precise determination of T_c in those superconductors with a tiny $\mu_0 H_{c1}(0)$. The consistency of the bulk and resistive T_c s suggest a good homogeneity of our samples.

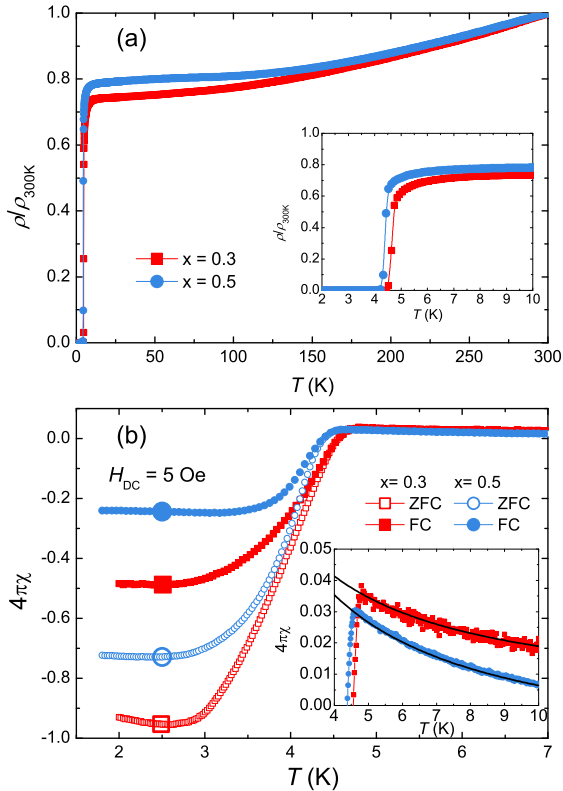


FIG. 1. (Color online) Temperature dependence of (a) the electrical resistivity normalized to its value at room temperature, $\rho(T)/\rho_{300K}$, and (b) the magnetic susceptibility $4\pi\chi(T)$ measured in zero-field cooling (ZFC) and field-cooling (FC) for the single crystalline $\text{NdO}_{1-x}\text{F}_x\text{BiS}_2$ ($x = 0.3$ and 0.5). The insets expand the portions near the superconducting transition. The magnetic susceptibility in the normal state shows a weak decrease above T_c , which follows the Curie behavior as demonstrated by the solid lines.

From the inset of Fig. 2, one can see that $\Delta f(T)$ for $x = 0.3$ and 0.5 shows a pronounced upturn as temperature goes to zero. Similar behavior was previously observed in $\text{Nd}_{2-x}\text{Ce}_x\text{CuO}_{4-\delta}$ ^{20,21} and $\text{NdFeAsO}_{0.9}\text{F}_{0.1}$ ²², which was attributed to the paramagnetic contributions of the Nd^{3+} ions. For superconductors with a significant paramagnetic background, the magnetic susceptibility in the Meissner state can be written as²²: $4\pi\chi(T) = [\sqrt{\mu(T)}\lambda_L(T)/R] \times \tanh[\sqrt{\mu(T)}R/\lambda_L(T)] - 1$, where $\lambda_L(T)$ is the London penetration depth, $\mu(T)$ is the normal-state paramagnetic permeability, and R is a characteristic sample dimension. In this case, screening of magnetic field is described by the London equation with an effective penetration depth $\lambda(T, \mu) = \lambda_L(T)\sqrt{\mu(T)}$, and the frequency shift $\Delta f(T)$ is proportional to $\Delta\lambda(T, \mu)$ rather than the $\Delta\lambda_L(T)$, i.e.,²¹

$$\Delta\lambda(T, \mu) = \Delta\lambda_L(T)\sqrt{\mu(T)} = G \cdot \Delta f(T). \quad (1)$$

In this context, we assume that the magnetic susceptibility of Nd^{3+} ions follows the same Curie law as in the normal state, i.e., $\chi(T) = \mu(T) - 1 = C/T$, which can reasonably describe the upturn of the frequency shift $\Delta f(T)$ in the low temperature limit (see the inset of Fig. 2). For superconductors with an isotropic energy gap (s -wave) or a nodal gap structure, the effective penetration depth $\lambda(T)$ in the presence of paramagnetic contributions takes the following expressions at $T \ll T_c$:²²

$$\lambda(T) = \sqrt{\mu(T)}\lambda(0)\left[1 + \sqrt{\frac{\pi\Delta(0)}{2k_B T}} \exp\left(-\frac{\Delta(0)}{k_B T}\right)\right], \quad (2)$$

or

$$\lambda(T) = \sqrt{\mu(T)}\lambda(0)[1 + AT^n], \quad (3)$$

where $n = 1$ and 2 correspond to the cases of line nodes and point nodes in the superconducting energy gap, respectively.

In Fig. 3, the symbols plot the temperature dependence of the effective penetration depth $\Delta\lambda(T)$ for $\text{NdO}_{1-x}\text{F}_x\text{BiS}_2$,

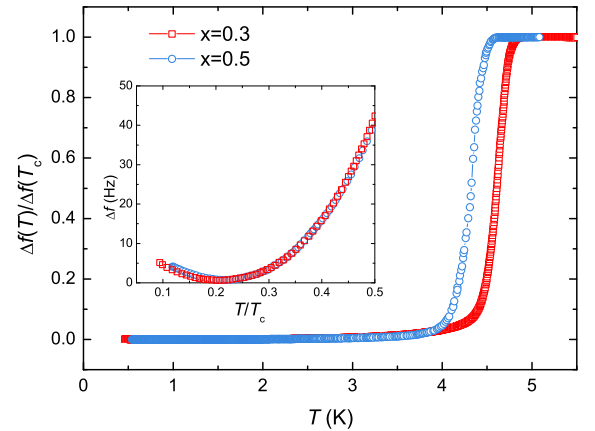


FIG. 2. (Color online) Temperature dependence of the frequency shift, $\Delta f(T)/\Delta f(T_c)$, normalized by its value at T_c for $\text{NdO}_{1-x}\text{F}_x\text{BiS}_2$ single crystals ($x = 0.3$ and 0.5). The inset shows the frequency shift $\Delta f(T)$ at low temperatures, which shows an upturn with decreasing temperature.

which are converted from the frequency shift $\Delta f(T)$ with $G = 7.4 \text{ \AA/Hz}$ and 7.8 \AA/Hz for $x = 0.3$ and 0.5 , respectively. The solid, dashed and dotted lines represent the fits of nodeless BCS model (Eq. 2) and nodal gaps with line ($n = 1$) and point nodes ($n = 2$), respectively. By taking $\lambda(0)$ as a free parameter, the fits of our experimental data to Eq. 2 give $\lambda(0) = 464 \text{ nm}$ and 436 nm for $x = 0.3$ and 0.5 , which are comparable to that of $\text{LaO}_{0.5}\text{F}_{0.5}\text{BiS}_2$ [$\lambda(0) = 484 \text{ nm}$] obtained from the μSR measurements¹⁶. From Fig. 3, one can see that the quadratic ($n = 2$) and linear ($n = 1$) temperature dependence of the London penetration depth (Eq. 3) fail to describe the experimental data, thus excluding the possibility of nodal SC. Instead, the BCS model (Eq. 2) fits nicely to the experimental data of both $x = 0.3$ and 0.5 ; the fitting parameters are summarized in Table I. The derived superconducting gaps are $\Delta(0) = 2.01 k_B T_c$ and $2.00 k_B T_c$ for $x = 0.3$ and 0.5 , respectively. These values are close to that of $\text{Bi}_4\text{O}_4\text{S}_3$ and LaOFBiS_2 obtained from the μSR experiments¹⁵, but significantly larger than that in the weak-coupling limit ($\Delta(0) = 1.76 k_B T_c$), indicating strong coupling SC in $\text{NdO}_{1-x}\text{F}_x\text{BiS}_2$.

To further analyze the gap symmetry, we derive the superfluid density $\rho_s(T)$ from the corresponding London penetration depth via $\rho_s(T) = \lambda(0)^2/\lambda_L(T)^2$ (see Fig. 4), where $\lambda_L(T)$ is obtained after subtracting the paramagnetic contributions. In general, the normalized superfluid density can be calculated

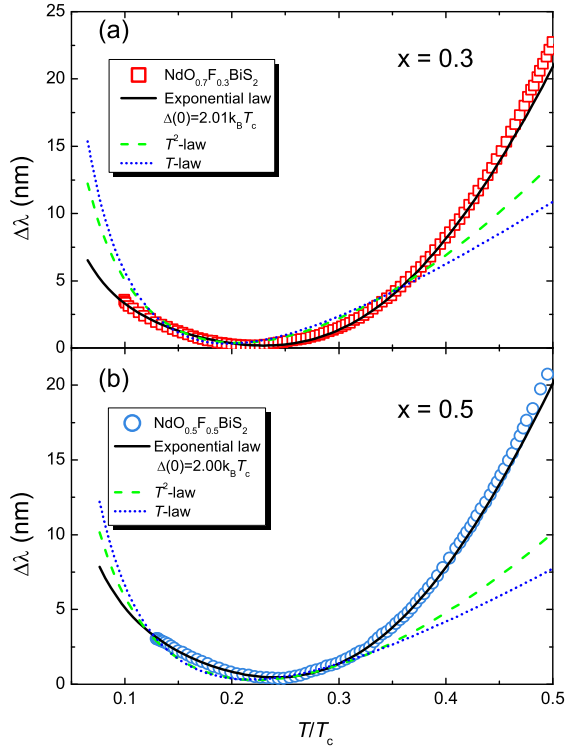


FIG. 3. (Color online) The change of effective penetration depth $\Delta\lambda(T)$ at low temperatures for $\text{NdO}_{1-x}\text{F}_x\text{BiS}_2$: (a) $x = 0.3$ (a); (b) $x = 0.5$. The solid lines are fits to Eq. 1, while the dashed- and dotted-lines represent fits to Eq. 2 with $n=1$ and 2 , respectively.

by:¹⁸

$$\rho_s(T) = 1 + 2 \langle \int_0^\infty \frac{\partial f}{\partial E} \frac{E}{\sqrt{E^2 - \Delta_k^2(T)}} dE \rangle_{\text{FS}}, \quad (4)$$

where $f = (e^{\sqrt{E^2 + \Delta_k^2(T)}/k_B T} + 1)^{-1}$ is the Fermi distribution function and $\langle \dots \rangle_{\text{FS}}$ denotes the average over the Fermi surface. As an approximation, we assume that the energy gap $\Delta(T)$ follows the BCS-type temperature dependence:¹⁸

$$\Delta(T) = \Delta(0) \tanh\{1.82[1.018(\frac{T_c}{T} - 1)^{0.51}]\} \Delta_k, \quad (5)$$

where $\Delta(0)$ is the energy gap at zero temperature. Given a gap function $\Delta_k [= \Delta(\theta, \varphi)]$ where θ and φ denote the polar angle and azimuthal angle, one can calculate the superfluid density $\rho_s(T)$ and fit it to the experimental data. In Fig. 4, three different gap functions are used to fit the experimental data $\rho_s(T)$, i.e., (i) s -wave: $\Delta(\theta, \varphi) = 1$; (ii) d -wave: $\Delta(\theta, \varphi) = \cos(2\varphi)$ and (iii) p -wave: $\Delta(\theta, \varphi) = |\sin(\theta)|$. One can see that the experimental data $\rho_s(T)$ can be well described by the BCS model but apparently deviate from the fits of the other two models with nodes in the gap structure, providing further evidence of BCS-like superconductivity for $\text{NdO}_{1-x}\text{F}_x\text{BiS}_2$. The derived superconducting energy gaps $\Delta(0)$ are listed in Table I, which are compatible with those derived in the preceding analysis of the magnetic penetration depth $\lambda(T)$. It is noted that, for $x = 0.5$, the fit of BCS model shows a small deviation from the experimental data $\rho_s(T)$ for $T > 0.6T_c$. At this stage, we cannot

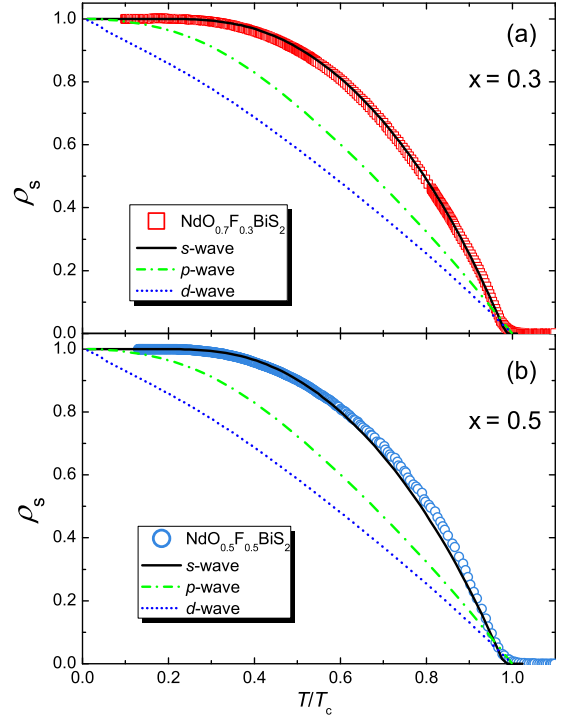


FIG. 4. (Color online) The normalized superfluid density $\rho_s(T)$ for $\text{NdO}_{1-x}\text{F}_x\text{BiS}_2$: (a) $x = 0.3$ and (b) $x = 0.5$ (b). The experimental data are fitted by various gap functions, i.e., s -wave SC (solid line), p -wave (dash-dotted line) and d -wave (dotted line).

TABLE I. The superconducting parameters of $\text{NdO}_{1-x}\text{F}_x\text{BiS}_2$.

x	$T_c(\text{K})$	$\lambda_L(0)$	$\Delta(0)$ by λ	$\Delta(0)$ by ρ_s	C	μ_{eff}
	K	nm	$k_B T_c$	$k_B T_c$	K	μ_B
0.3	4.5	464	2.01	2.20	0.0123	0.31
0.5	4.2	436	2.00	2.15	0.0167	0.37

exclude the possibility of anisotropic or multiband superconductivity for $x = 0.5$ which may fit better to the experimental data (with more fitting parameters). On the other hand, such a small deviation might be caused by some uncertainties of the derived λ_0 and the G -factor too.

The above analyses of the magnetic penetration depth $\Delta\lambda(T)$ and the corresponding superfluid density $\rho_s(T)$ have shown BCS-type superconductivity for $\text{NdO}_{1-x}\text{F}_x\text{BiS}_2$ ($x = 0.3$ and 0.5). In a conventional s -wave superconductor, T_c can be rapidly suppressed by magnetic impurities²³. Thus, the appearance of a BCS-like SC in the presence of localized magnetic moments of Nd ions is unusual. Indeed, evidence of nodal gap superconductivity was obtained for the Nd-based superconductors $\text{Nd}_{2-x}\text{Ce}_x\text{CuO}_{4-\delta}$ ^{20,21} and $\text{NdFeAsO}_{0.9}\text{F}_{0.1}$ ²². Recently, it was theoretically proposed that, as a result of strong spin-orbit coupling, a dominant spin-triplet state may coexist with a spin-singlet component in the BiS_2 -based superconductors, resulting in a crossover from nodeless SC to nodal SC with increasing the electron filling above a so-called Lifshitz point¹³. If such a theoretical scenario is valid, then our results suggest that the filling level

of $\text{NdO}_{0.5}\text{F}_{0.5}\text{BiS}_2$ is still below the Lifshitz point, and nodal SC would be expected with further increasing the F-doping concentration, which might push the Fermi level close to a van Hove singularity. Indeed, the recent ARPES experiments revealed that the deficiency of Bi element in $\text{NdO}_{1-x}\text{F}_x\text{BiS}_2$ may result in a reduction of the actual filling level,^{24,25} meaning that the samples with $x = 0.5$ are likely below the Lifshitz point. Therefore, it is highly desired to systematically study the samples with higher doping concentrations. Unfortunately, the growth of single crystals with rich F-content has not been successful yet and further efforts are badly needed.

In summary, we have performed measurements of magnetic penetration depth $\Delta\lambda(T)$ for the $\text{NdO}_{1-x}\text{F}_x\text{BiS}_2$ ($x = 0.3$ and 0.5) single crystals by utilizing a TDO-based technique down to 0.4 K. Strong evidence of BCS-like SC with a large gap size is found in both the low-temperature penetration depth $\lambda(T)$ and its corresponding superfluid density $\rho_s(T)$. A Curie-like paramagnetic contribution of Nb^{3+} shows up in the superconducting state which is rare in a BCS-like superconductor. Future works are needed to clarify the gap structure in the overdoped region and, therefore, to test the currently available theories.

We are grateful to Q. H. Wang and C. Cao for helpful discussions. This work was supported by the National Basic Research Program of China (No. 2011CBA00103), the National Nature Science Foundation of China (No. 11174245) and the Fundamental Research Funds for the Central Universities.

* hqyuan@zju.edu.cn

- ¹ Y. Mizuguchi, H. Fujihisa, Y. Gotoh, K. Suzuki, H. Usui, K. Kuroki, S. Demura, Y. Takano, H. Izawa, O. Miura, Phys. Rev. B **86**, 220510(R) (2012).
- ² S. K. Singh, A. Kumar, B. Gahtori, Shruti, G. Sharma, S. Patnaik, and V. P. S. Awana, J. Am. Chem. Soc. **134**, 16504 (2012).
- ³ Y. Mizuguchi, S. Demura, K. Deguchi, Y. Takano, H. Fujihisa, Y. Gotoh, H. Izawa, and O. Miura, J. Phys. Soc. Jpn. **81**, 114725 (2012).
- ⁴ R. Jha, A. Kumar, S. Kumar Singh, and V. P. S. Awana, J. Supercond. Novel Magn. **26**, 499 (2013).
- ⁵ S. Demura, et al., J. Phys. Soc. Jpn. **82**, 33708 (2013).
- ⁶ D. Yazici, K. Huang, B. D. White, A. H. Chang, A. J. Friedman, and M. B. Maple, Philos. Mag. **93**, 673 (2013).
- ⁷ J. Xing, S. Li, X. Ding, H. Yang, and H. H. Wen, Phys. Rev. B **86**, 214518 (2012).
- ⁸ J. Liu, D. Fang, Z. Wang, J. Xing, Z. Du, X. Zhu, H. Yang, and H. H. Wen, EPL **106**, 67002 (2014).
- ⁹ M. Nagao, S. Demura, K. Deguchi, A. Miura, S. Watauchi, T. Takei, Y. Takano, N. Kumada, and I. Tanaka, J. Phys. Soc. Jpn. **82**, 113701 (2013).
- ¹⁰ *Handbook of High-Temperature Superconductivity: Theory and Experiment*, edited by J. R. Schrieffer and J. S. Brooks (Springer Science, New York, 2007).
- ¹¹ For reviews, see, e.g., G. R. Stewart, Rev. Mod. Phys. **83**, 1589 (2011); J. Paglione and R. L. Greene, Nat. Phys. **6**, 645 (2010); D. C. Johnston, Adv Phys **59**, 803 (2010).
- ¹² T. Yildirim, Phys. Rev. B **87**, 20506 (2013).
- ¹³ Y. Yang, W. Wang, Y. Xiang, Z. Li, and Q. Wang, Phys. Rev. B **88**, 94519 (2013).
- ¹⁴ X. X. Wu, J. Yuan, Y. Liang, H. Fan, and J. P. Hu, arXiv:1403.5949.
- ¹⁵ P. K. Biswas, A. Amato, C. Baines, R. Khasanov, H. Luetkens, H. Lei, C. Petrovic, and E. Morenzoni, Phys. Rev. B **88**, 224515 (2013).
- ¹⁶ G. Lamura, et al., Phys. Rev. B **88**, 180509 (2013).
- ¹⁷ Shruti, P. Srivastava and S. Patnaik, J. Phys.: Condens. Matter **25**, 339601 (2013).
- ¹⁸ R. Prozorov and R. W. Giannetta, Supercond. Sci. Technol. **19**, R41 (2006).
- ¹⁹ R. Jha, A. Kumar, S. Kumar Singh, and V. P. S. Awana, J. Appl. Phys. **113**, 056102 (2013).
- ²⁰ J. D. Kokales, P. Fournier, L. V. Mercaldo, V. V. Talanov, R. L. Greene, and S. M. Anlage, Phys. Rev. Lett. **85**, 3696 (2000).
- ²¹ R. Prozorov, R. W. Giannetta, P. Fournier, and R. L. Greene, Phys. Rev. Lett. **85**, 3700 (2000).
- ²² C. Martin, et al., Phys. Rev. Lett. **102**, 247002 (2009).
- ²³ A. A. Abrikosov and L. P. Gor'kv, Societ Phys. JETP **12**, 1243 (1961).
- ²⁴ Z. R. Ye, H. F. Yang, D. W. Shen, J. Jiang, X. H. Niu, D. L. Feng, Y. P. Du, X. G. Wan, J. Z. Liu, X. Y. Zhu, H. H. Wen, and M. H. Jiang, arXiv:1402.2860.
- ²⁵ L. K. Zeng, X. B. Wang, J. Ma, P. Richard, S. M. Nie, H. M. Weng, N. L. Wang, Z. Wang, T. Qian, and H. Ding, arXiv:1402.1833.